Rate and Mechanism of the Reaction of (*E*)-PhCH=CH-CH(Ph)-OAc with Palladium(0) Complexes in Allylic Substitutions

Christian Amatore,*,† Ali A. Bahsoun,† Anny Jutand,*,† Laure Mensah,† Gilbert Meyer,† and Louis Ricard‡

Département de Chimie, Ecole Normale Supérieure, UMR CNRS-ENS-UPMC 8640, 24 Rue Lhomond, F-75231 Paris Cedex 5, France, and Ecole Polytechnique, DCPH, UMR CNRS 7653, F-91128 Palaiseau, France

Received July 27, 2004

The reaction of (*E*)-1,3-diphenyl-3-acetoxyprop-1-ene, PhCH=CH−CH(Ph)-OAc, with palladium(0) complexes Pd^0L_2, generated from $Pd^0(PPh_3)_4$ or $Pd^0(dba)_2$ + 2L (L = PPh_3 or L_2 = dppb), gives cationic $[(\eta^3\text{-PhCH-CH-CHPh})PdL_2]^+$ complexes with AcO^- as the counteranion in DMF. It is established that this reaction proceeds through two successive equilibria via neutral intermediate complexes $(\eta^2\text{-PhCH=CH-CH(Ph)-OAc})Pd^0L_2$, characterized from the kinetics and by UV and ^{31}P NMR spectroscopy. The rate constants and equilibrium constants of the successive steps have been determined in DMF. They depend on the ligand and the Pd^0 precursor. In all cases, for the concentration range investigated here, the complexation is considerably faster than the ionization, which is the rate-determining step of the overall process. Under similar experimental conditions, the formation of the cationic complex $[(\eta^3\text{-PhCH-CH-CHPh})Pd(dppb)]^+$ is considerably slower than the formation of the complex $[(\eta^3\text{-CH}_2\text{-CH-CH}_2)Pd(dppb)]^+$ in DMF.

Introduction

The (*E*)-1,3-diphenyl-3-acetoxyprop-1-ene (**1**) is often used as a model molecule in enantioselective palladium-catalyzed nucleophilic allylic substitutions (eq 1).[1]

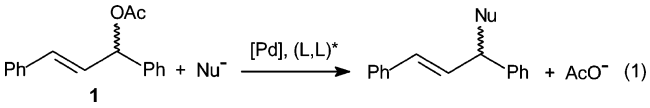

The postulated mechanism involves an oxidative addition of the racemic substrate **1** to a chiral Pd^0 complex, which generates, in the case of a C_2-symmetric chiral ligand, one single cationic complex $[(\eta^3\text{-1,3-diphenylallyl})Pd(L,L)^*]^+$, $\mathbf{2}^+$, due to the symmetry of the allyl moieties (Scheme 1). The regioselectivity of the nucleophilic attack is at the origin of the enantioselectivity of the catalytic reaction.[1] The introduction of a functional group on the chiral ligand that can interact with the nucleophile may generate an enhanced center for the nucleophilic attack on the allylic moieties.[1g−i] A steric repulsion between one phenyl group of the allylic ligand and the chiral ligand in complex $\mathbf{2}^+$ may result in a longer Pd−C bond, which favors the nucleophilic attack at this carbon, as evidenced for chiral *N*,*N*-bis(oxazoline) ligands.[1j] Stacking of the phenyl group of the 1,3-diphenylallyl ligand with the phenyl group of chiral P,P ligands has also been observed.[1q]

Scheme 1

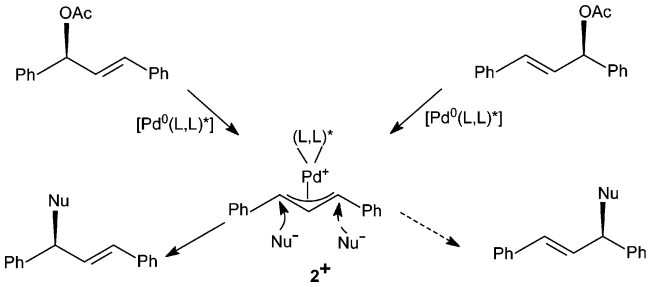

The enantioselectivity may also be related to the thermodynamic stability of the intermediate $(\eta^2\text{-PhCH=CH-CH(Ph)-Nu})Pd^0(L,L)^*$ complexes[1j,t] generated in the nucleophilic attack on the cationic complex $\mathbf{2}^+$. In the case of chiral P,N ligands such as phosphinooxazolines, one major *exo* diastereoisomer is formed.[1k,m] The regio-

* Corresponding authors. Fax: 33 1 44 32 33 25. E-mail: Anny.Jutand@ens.fr; christian.amatore@ens.fr.
† Ecole Normale Supérieure.
‡ Ecole Polytechnique.

(1) (a) Godleski S. A. In *Comprehensive Organic Synthesis*, *Vol. 4*; Trost, B. M., Pflemming, I., Semmelhack, M. F., Eds.; Pergamon: Oxford, 1991. (b) Frost, C. G.; Howard, J.; Williams, J. M. J. *Tetrahedron Asymmetry* **1992**, *3*, 1089. (c) Tsuji, J. *Palladium Reagents and Catalysts*; John Wiley & Sons: Chichester, 1996; p 290. (d) Trost, B. M.; Van Kanken, D. L. *Chem. Rev.* **1996**, *96*, 395. (e) Auburn, P. R.; Mackenzie, P. B.; Bosnich, B. *J. Am. Chem. Soc.* **1985**, *107*, 2033. (f) Consiglio, G.; Waymouth, R. *Chem. Rev.* **1989**, *89*, 257. (g) Hayashi, T. *Pure Appl. Chem.* **1988**, *60*, 7. (h) Hayashi, T.; Yamamoto, A.; Ito, Y.; Nishioha, E.; Miura, H.; Yanagi, K. *J. Am. Chem. Soc.* **1989**, *111*, 6301. (i) Sawamura, M.; Ito, Y. *Chem. Rev.* **1992**, *92*, 857. (j) Pfaltz, A. *Acc. Chem. Rev.* **1993**, *26*, 339. (k) Baltzer, N.; Macko, L.; Schaffner, S.; Zehnder, M. *Helv. Chim. Acta* **1996**, *79*, 803. (l) Helmchen, G.; Pfaltz, A. *Acc. Chem. Res.* **2000**, *33*, 336. (m) Markert, C.; Pfaltz, A. *Angew. Chem., Int. Ed.* **2004**, 43, 2498. (n) Togni, A.; Burckhardt, U.; Gramlich, V.; Pregosin, P. S.; Salzman, R. *J. Am. Chem. Soc.* **1996**, *118*, 1031. (o) Pregosin, P. S.; Salzman, R. *Coord. Chem. Rev.* **1996**, *155*, 36. (p) Pregosin, P. S.; Salzman, R. *Organometallics* **1999**, *18*, 1207−1215. (q) Barbaro, P.; Pregosin, P. S.; Salzman, R.; Albinati, A.; Kunz, R. W. *Organometallics* **1995**, *14*, 5160. (r) Herrmann, J.; Pregosin, P. S.; Salzman, R.; Albinati, A. *Organometallics* **1995**, *14*, 3311. (s) Burckhardt, U.; Gramlich, V.; Hofmann, P.; Nesper, R.; Pregosin, P. S.; Salzman, R.; Togni, A. *Organometallics* **1996**, *15*, 3496. (t) Steinhagen, H.; Reggelin, S.; Helmchen, G. *Angew. Chem., Int. Ed. Engl.* **1997**, *36*, 2108.

10.1021/om049420d CCC: $30.25
Publication on Web 02/25/2005

Scheme 2[a]

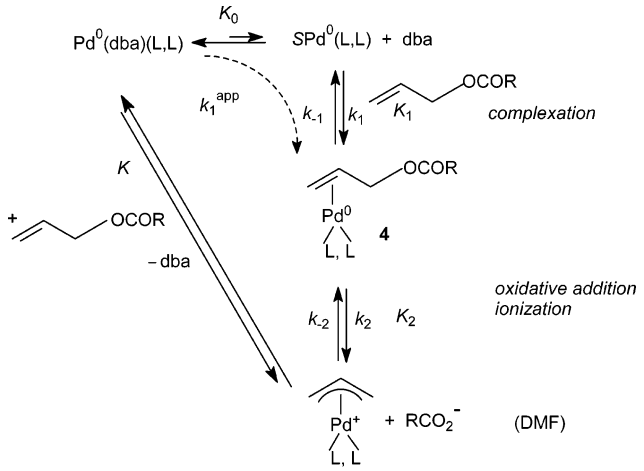

[a] L,L means either two PPh_3 or one bidentate bisphosphine ligand: dppb or dppf.

selectivity and consequently the enantioselectivity are improved since the nucleophilic attack mainly occurs at the allylic carbon *trans* to the phosphorus atom. This specific attack has been observed for a series of chiral P,N ligands.[1m,p,q,s]

The formation of the cationic complex in the reaction of racemic **1** with Pd^0 complexes is usually considered to be fast and irreversible and the nucleophilic attack slower and turnover limiting.[1j,l,m]

It has been established that the reaction of allyl carboxylates[2] or carbonates[3] to $Pd^0(L,L)$ complexes ligated by either two monodentate PPh_3[2a,c,d] or one bidentate P,P ligand (dppb, dppf)[2b–d] is reversible and proceeds in two successive reversible steps (Scheme 2).

However, the existence of the intermediate neutral Pd^0 complexes **4** formed in the complexation step (Scheme 2) was established from kinetic data only.[2b] None of them had been characterized by the usual spectroscopic techniques (NMR, UV, etc.) due to too short lifetimes.

We report herein an investigation on the rate and mechanism of the reaction of (*E*)-1,3-diphenyl-3-acetoxyprop-1-ene (**1**) to Pd^0 complexes ligated by PPh_3 (as representative of monodentate ligands) or dppb (1,4-bis(diphenylphosphino)butane, as representative of bidentate symmetrical P,P ligands), which establishes that the overall reaction is reversible and proceeds in two steps from Pd^0L_2 complexes. In addition, the existence of the intermediate complexes (η^2-PhCH=CH-CH(Ph)OAc)Pd^0L_2 was confirmed by UV and ^{31}P NMR spectroscopy.

Results and Discussion

Reaction of (*E*)-1,3-Diphenyl-3-acetoxyprop-1-ene (1) with the Pd^0 Complex Generated from $Pd^0(dba)_2$ and $2PPh_3$. Evidence of the Reversibility of the Oxidative Addition. $Pd^0(dba)_2$ associated with 2 equiv of PPh_3[5] quantitatively generates $Pd^0(dba)(PPh_3)_2$ as the major but unreactive complex in DMF.[6] The oxidative addition of allylic carboxylates proceeds from the minor reactive complex $SPd^0(PPh_3)_2$ and is known to generate the cationic complex $[(\eta^3\text{-allyl})Pd(PPh_3)_2]^+$ (Scheme 2).[2a] The formation of the cationic complex **5a**$^+$ in the reaction of **1** with $Pd^0(dba)(PPh_3)_2$ is therefore expected (eq 2).

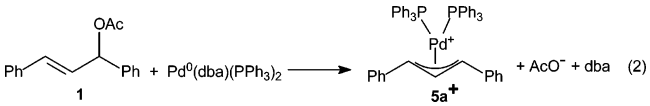

This complex **5a**$^+$OAc$^-$ has indeed been observed by ESI-MS analysis in the course of a catalytic allylic substitution performed on **1**.[7a] The complex **5a**$^+BF_4^-$ was synthesized independently from the dimeric complex[7b] $[(\eta^3\text{-}1,3\text{-diphenylallyl})Pd(\mu\text{-Cl})]_2$ by addition of PPh_3 (PPh_3/Pd = 2) in the presence of $NaBF_4$ (eq 3).[7c] It was characterized by an X-ray structure study (Figure 1, Table 1).

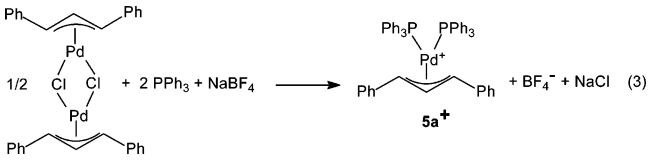

The reaction of complex **5a**$^+BF_4^-$ (1 mM) with 1 equiv of nBu$_4$NOAc and 2 equiv of dba was monitored by ^{31}P

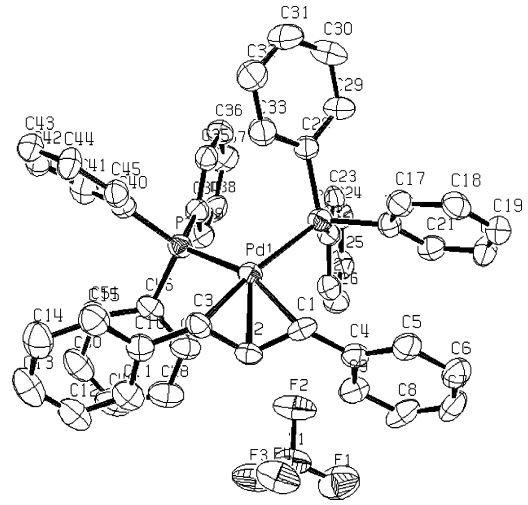

Figure 1. X-ray structure of $[(\eta^3\text{-PhCH-CH-CHPh})Pd(PPh_3)_2]^+BF_4^-$ (**5a**$^+BF_4^-$).

(2) (a) Amatore, C.; Jutand, A.; Meyer, G.; Mottier, L. *Chem. Eur. J.* **1999**, *5*, 466. (b) Amatore, C.; Gamez, S.; Jutand, A. *Chem. Eur. J.* **2001**, *7*, 1273. (c) Amatore, C.; Gamez, S.; Jutand, A.; Meyer, G.; Mottier, L. *Electrochim. Acta* **2001**, *46*, 3237. (d) Agenet, N.; Amatore, C.; Gamez, S.; Gérardin, H.; Jutand, A.; Meyer, G.; Orthwein, C. *ARKIVOC* **2002**, 92. http://www.arkat-usa.org/.

(3) Amatore, C.; Gamez, S.; Jutand, A.; Meyer, G.; Moreno-Mañas, M.; Morral, L.; Pleixats, R. *Chem. Eur. J.* **2000**, *6*, 3372.

(4) For the use of conductivity measurements for the determination of mechanisms see: Jutand, A. *Eur. J. Inorg. Chem.* **2003**, 2017.

(5) (a) For seminal works on the use of $Pd(dba)_2$ with monodentate phosphine ligands in allylic substitutions, see: Ferroud, D.; Genêt, J. P.; Muzart, J. *Tetrahedron Lett.* **1984,** *25,* 4379. (b) For seminal works on the use of $Pd(dba)_2$ with bidentate phosphine ligands in allylic substitutions, see: Fiaud, J. C.; Hibon de Gournay, A.; Larchevêque, M.; Kagan, H. B. *J. Organomet. Chem.* **1978,** *154,* 175.

(6) (a) Amatore, C.; Jutand, A.; Khalil, F.; M'Barki, M. A.; Mottier, L. *Organometallics* **1993**, *12*, 3168. (b) Amatore, C.; Jutand, A.; Meyer, G. *Inorg. Chim. Acta* **1998**, *273*, 76. (c) Amatore, C.; Jutand, A. *Coord. Chem. Rev.* **1998**, *178–180*, 511.

(7) (a) Chevrin, C.; Le Bras, J.; Hénin, F.; Muzart, J. Pla-Quintana, A.; Roglans, A.; Pleixats, R. *Organometallics* **2004**, 23, 4796–4799. (b) The dimer $[Pd(\eta^3\text{-PhCH-CH-CHPh})(\mu\text{-Cl})]_2$ was synthesized according to a reported procedure[1h] but from Na_2PdCl_4. (b) The cationic complex with BF_4^- as the counteranion was synthesized as in ref 2a with a procedure similar to that reported for BPh_4^- as the counteranion: Powell, J.; Shaw, B. L. *J. Chem. Soc. (A)* **1968**, 774.

Table 1. Crystal Data for [(η^3-PhCH-CH-CHPh)Pd(PPh$_3$)]$^+$BF$_4^-$ (5a$^+$BF$_4^-$)

molecular formula	$C_{51}H_{43}BF_4P_2Pd$
molecular wt	911.00
cryst habit	pale orange block
cryst dimens (mm)	0.20 × 0.20 × 0.20
cryst syst	orthorhombic
space group	*Pbca*
a (Å)	19.5620(10)
b (Å)	19.5850(10)
c (Å)	44.0770(10)
α (deg)	90.00
β (deg)	90.00
γ (deg)	90.00
V (Å^3)	16886.9(13)
Z	16
d (g cm^{-3})	1.433
*F*000	7456
μ (cm^{-1})	0.569
absorp corr	multiple scans; 0.8947 min., 0.8947 max.
diffractometer	KappaCCD
X-ray source	Mo Kα
λ (Å)	0.71069
monochromator	graphite
T (K)	150.0(10)
scan mode	phi and omega scans
maximum *θ*	23.81
hkl ranges	−22 19; −22 22; −49 49
no. of reflns measd	50 716
unique data	12 532
R_{int}	0.0641
no. of reflns used	9106
criterion	>2*σ*(*I*)
refinement type	*F*^{2}
hydrogen atoms	mixed
no. of params refined	1073
no. of reflns/params	8
wR2	0.1615
R1	0.0527
weights a, b	0.1044; 0.0000
GoF	1.040
diff peak/hole (e/Å^{-3})	1.293(0.101)/−1.197(0.101)

NMR spectroscopy in DMF containing 10% acetone-d_6. The singlet characterizing **5a**$^+$BF$_4^-$ at 27.8 ppm disappeared, whereas two broad signals at 26.7 and 24.8 ppm corresponding to Pd^0(dba)(PPh$_3$)$_2$ appeared. This established the reversibility of eq 2, i.e., that the acetate ion reacts with the cationic complex **5a**$^+$ to eventually generate a Pd^0 complex (reverse reaction in eq 4).

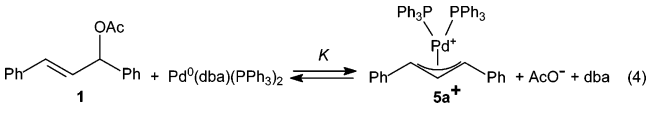

The same reaction was monitored by UV spectroscopy in DMF. The absorption band of the cationic complex **5a**$^+$BF$_4^-$ (1 mM) at λ_{max} = 350 nm disappeared while the absorption band at λ_{max} = 395 nm characteristic of Pd^0(dba)(PPh$_3$)$_2$ appeared (Figure 2a).

The forward reaction of the equilibrium in eq 4 was monitored by ^{31}P NMR spectroscopy. To a solution of Pd^0(dba)(PPh$_3$)$_2$ (20 mM), quantitatively formed in situ from Pd^0(dba)$_2$ and 2 equiv of PPh$_3$ in acetone-d_6,[6a] was added 88 equiv of **1**. After 1 h, the two broad singlets of Pd^0(dba)(PPh$_3$)$_2$ at 25.4 and 27.3 ppm were still detected, but two new doublets of equal magnitude had appeared at 24.97 (d, J_{PP} = 23 Hz, 1P) and 24.61 ppm (d, J_{PP} = 23 Hz, 1P). After one night, Pd^0(dba)(PPh$_3$)$_2$ was no longer detected, the two new doublets were still present together with a minor thin singlet at 27.8 ppm

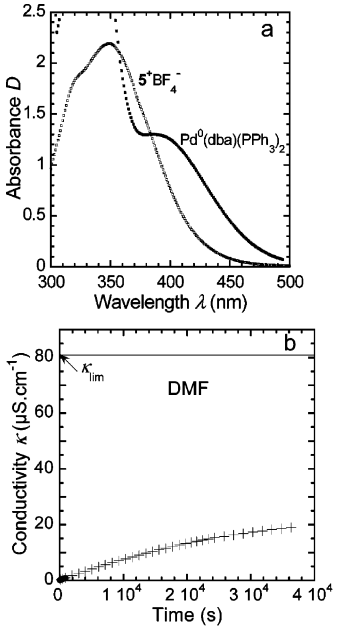

Figure 2. (a) UV spectroscopy performed in DMF in a 1 mm length cell at room temperature: (open squares) [(η^3-PhCH-CH-CHPh)Pd(PPh$_3$)$_2$]$^+$BF$_4^-$ (**5a**$^+$BF$_4^-$) (1 mM); (full squares) Pd^0(dba)(PPh$_3$)$_2$ generated by addition of 10 equiv of *n*Bu$_4$NOAc and 2 equiv of dba to **5a**$^+$BF$_4^-$ (1 mM). (b) Conductivity measurements in DMF versus time of [(η^3-PhCH-CH-CHPh)Pd(PPh$_3$)$_2$]$^+$AcO$^-$ (**5a**$^+$AcO$^-$) generated in the reaction of PhCH=CH-CH(Ph)-OAc (88.6 mM) (+) or (200 mM) (•) to Pd^0(dba)(PPh$_3$)$_2$ (1 mM) formed in situ by reacting Pd^0(dba)$_2$ (1 mM) and PPh$_3$ (2 mM) at 25 °C. κ_{lim} is the theoretical conductivity of **5a**$^+$AcO$^-$ (1 mM) in DMF at 25 °C.[8a]

Scheme 3

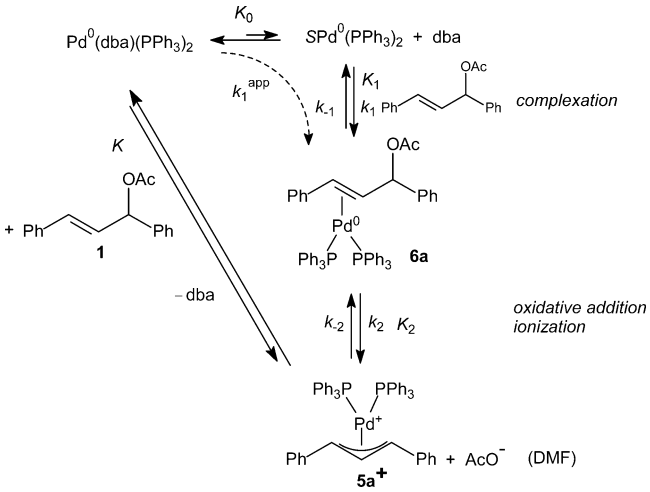

characteristic of the cationic complex **5a**$^+$. The magnitude of the latter singlet increased with time at the expenses of that of the two doublets. The cationic complex **5a**$^+$ was never observed alone, even at very long times (5 days in DMF). Consequently, the reaction of Pd^0(dba)(PPh$_3$)$_2$ with **1** gave the expected cationic complex **5a**$^+$ via an intermediate complex containing two non magnetically equivalent phosphines as expected for (η^2-PhCH=CH-CH(Ph)-OAc)Pd^0(PPh$_3$)$_2$, **6a** (Scheme 3). This experiment establishes the existence of two successive steps, presumably complexation and ionization, during the reaction of **1** with *S*Pd^0(PPh$_3$)$_2$ (Scheme 3).

Under our experimental conditions, the complexation step was faster than the ionization step. The intermediate Pd^0 complex **6a** could thus be accumulated and characterized. To the best of our knowledge, this is the first spectroscopic characterization of a Pd^0 complex ligated by the C=C bond of an allylic carboxylate. The complex **6a** could not be characterized by ^1H NMR spectroscopy because it was generated in the presence of a large amount of **1** (88 equiv with respect to **6a**).

The forward reaction of the equilibrium in eq 4 was monitored by conductivity measurements[4] to detect the formation of the cationic complex $\mathbf{5a}^+$ (Figure 2b). To a solution of $Pd^0(dba)(PPh_3)_2$ (1 mM), quantitatively formed from $Pd^0(dba)_2$ (1 mM) and 2 equiv of PPh_3 in DMF, was added the allylic acetate **1** in large excess (200 mM), i.e., producing conditions in which a fast irreversible complexation was observed between $Pd^0(dba)(PPh_3)_2$ and **1** ($t_{1/2} < 1$ s). The conductivity slowly increased with time (Figure 2b). It never stabilized within the time scale investigated here and never reached the value of $\kappa_{lim} = 81\ \mu S\ cm^{-1}$ (Figure 2b), which is the theoretical conductivity of $\mathbf{5a}^+AcO^-$ (1 mM) in DMF corresponding to 100% conversion, as determined independently.[8a] In DMF, the cationic complex $\mathbf{5a}^+BF_4^-$ ($C_0 = 1$ mM) partially disappeared in a fast reaction upon addition of AcO^- ($C_0 = 1$ mM), which implies that $k_{-2}[AcO^-] > k_2$. Consequently, at the concentration of $C_0 = 1$ mM used in Figure 2b, one cannot observe the quantitative formation of $\mathbf{5a}^+AcO^-$. What is observed in Figure 2b is then the slow ionization of the intermediate complex **6a** to the cationic complex $\mathbf{5a}^+$ in a reversible step (Scheme 3) without reaching its equilibrium position.

It is then confirmed that in the presence of a large excess of **1** ($C > 0.03$ M) the intermediate neutral complex **6a** was generated in a fast reaction, which is followed by a slower ionization.

Complexation Step: Kinetic and Thermodynamic Data. In DMF at 25 °C, the absorbance[6b] of $Pd^0(dba)(PPh_3)_2$ ($C_0 = 1$ mM) partly decreased in a fast reaction (occurring during mixing) and stabilized in the presence of various amounts of **1** (nC_0) added successively (Figure 3a). This attests that $Pd^0(dba)(PPh_3)_2$ and the allylic acetate **1** were involved in an equilibrium with the intermediate complex **6a** since the latter accumulated due to its very slow ionization to $\mathbf{5a}^+$ (as evidenced above by conductivity measurements). The equilibrium constant $K_0K_1 = [\mathbf{6a}][dba]/[\mathbf{1}][Pd^0(dba)(PPh_3)_2]$ of the overall complexation step (Scheme 4) was then determined (Table 2, entry 2, Figure S1a in the Supporting Information) using the UV data shown in Figure 3a, by neglecting the very slow ionization of **6a** within the experiment time.

The kinetics of the overall complexation step (see k_1^{app} in Scheme 3) was monitored by UV spectroscopy by recording the decrease of the absorbance of $Pd^0(dba)(PPh_3)_2$ ($C_0 = 0.99$ mM) versus time in the presence of large amounts of **1** ($nC_0 > 0.03$ M). Such conditions were designed to allow the observation of an overall irreversible complexation step. Taking into account the variation of the dba concentration during the reaction, the kinetic law is given in eq 5 (x is the molar fraction of $Pd^0(dba)(PPh_3)_2$ that has not reacted: $x = (D_n - D_\infty)/(D_0 - D_\infty)$ (D_0: initial absorbance of $Pd^0(dba)(PPh_3)_2$; D_n: absorbance of $Pd^0(dba)(PPh_3)_2$ at t in the presence of $n = 30$ equiv of **1**; D_∞: residual absorbance at the end of the complexation step).

$$2\ln x - x + 1 = -K_0k_1[\mathbf{1}]t/C_0 = -k_{exp}t = -k_1^{app}[\mathbf{1}]t \quad (5)$$

The plot of $2\ln x - x + 1$ versus time was linear (Figure S1b in the Supporting Information) and the experimental rate constant k_{exp} determined from the slope. The plot of k_{exp} versus the concentration of **1** was linear (Figure 3b) and went through zero, which demonstrates a first-order reaction in **1** (eq 5). The value of k_1^{app} was calculated from the slope in Figure 3b as well as the value of K_0k_1 (Table 2, entry 2). The value of k_{-1}

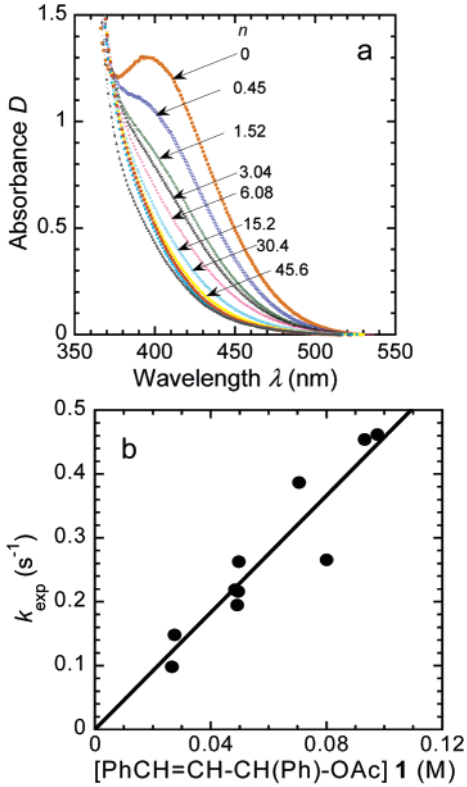

Figure 3. (a) UV spectroscopy performed in DMF in a 1 mm length cell at 25 °C of $Pd^0(dba)(PPh_3)_2$ (1 mM) (formed in situ by reacting $Pd^0(dba)_2$ (1 mM) and PPh_3 (2 mM)) after successive additions of PhCH=CH-CH(Ph)-OAc (**1**) (n is the total number of equivalents of **1** added to $Pd^0(dba)(PPh_3)_2$). (b) Kinetics of the overall complexation step (see k_1^{app} in Scheme 3) as monitored by UV spectroscopy in DMF at 25 °C. Determination of the reaction order in PhCH=CH-CH(Ph)-OAc: plot of k_{exp} versus PhCH=CH-CH(Ph)-OAc concentration. $k_{exp} = K_0k_1[\mathbf{1}]/C_0$, $k_1^{app} = 4.5\ M^{-1}\ s^{-1}$, and $K_0k_1 = 4.5 \times 10^{-3}\ s^{-1}$ (DMF, 25 °C).

Scheme 4. Overall Complexation Step

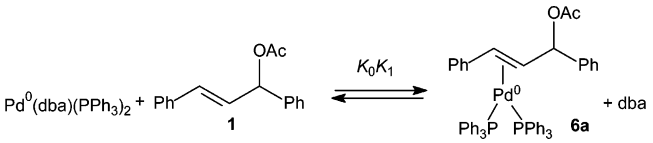

(8) (a) The theoretical conductivity κ of $\mathbf{5a}^+AcO^-$ (1 mM) in DMF was calculated from the measured conductivity $\kappa_1 = 66.7\ \mu S\ cm^{-1}$ of $nBu_4N^+AcO^-$ (1 mM), the conductivity $\kappa_2 = 102\ \mu S\ cm^{-1}$ of $\mathbf{5a}^+BF_4^-$ (1 mM), and the conductivity $\kappa_3 = 78\ \mu S\ cm^{-1}$ of $nBu_4N^+BF_4^-$ (1 mM) in DMF: $\kappa = \kappa_2 + \kappa_1 - \kappa_3 = 81\ \mu S\ cm^{-1}$ (κ_{lim} in Figure 2a). (b) The theoretical conductivity of $\mathbf{5a}^+AcO^-$ (1 mM) in acetonitrile (κ_{lim} in Figure S2a in Supporting Information) was independently calculated as in ref 8a.

Table 2. Equilibrium and Rate Constants for the Reaction of PhCH=CH-CH(Ph)-OAc with Pd^0 Complexes (C_0 = 1 mM) in DMF at 25 °C Except[a] at 30 °C (comparison with CH_2=CH-CH_2-OAc is given in entry 5[2b])

	Pd^0 precursor	$K = K_0K_1K_2$ (M)	K_0K_1	K_0k_1 (s^{-1})	k_1^{app} (M^{-1} s^{-1})	k_{-1} (s^{-1})	k_2 (s^{-1})	k_{-2} (M^{-1} s^{-1})
1	$Pd^0(PPh_3)_4$[b]	nd	8.7	2.3×10^{-2}	23	5×10^{-3}	1×10^{-5}	$\gg 10^{-2}$
2	$Pd^0(dba)_2$ + 2 PPh_3[c]	nd	0.19	4.5×10^{-3}	4.5	5×10^{-3}	1×10^{-5}	$\gg 10^{-2}$
3	$Pd^0(dba)_2$ + 2 PPh_3[c]						5.3×10^{-4} [d]	
4	$Pd^0(dba)_2$ + 1 dppb[e]	0.021	nd	5.3×10^{-4}	0.53	nd	3×10^{-4} [a]	$<3 \times 10^{-7}$ [a]
5	$Pd^0(dba)_2$ + 1 dppb[f]	0.018	nd	5.8×10^{-2}	58	nd	2.5×10^{-2}	nd

[a] 30 °C. [b] See Scheme 6 with $K_0 = K'_0$. [c] See Scheme 3. [d] In acetonitrile. [e] See Scheme 9. [f] Reaction with CH_2=CH-CH_2-OAc.[2b]

Scheme 5. Ionization Step

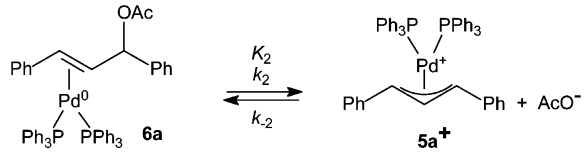

(Scheme 3) could then be deduced from the value of K_0K_1 determined above (Table 2, entry 2).

Ionization Step: Kinetic Data. As evidenced above (Figure 2a), the ionization step is reversible in DMF (Scheme 5). The rate of formation of the cationic complex **5a**$^+$ could be monitored by conductivity measurements versus time (Figure 2b), after addition of a large excess of **1** (88.6 or 200 mM) to $Pd^0(dba)(PPh_3)_2$ (C_0 = 1 mM) in DMF. Under these conditions, the formation of the intermediate complex **6a** was considerably faster than the ionization step and the slow equilibration of the ionization step was then observed in Figure 2b, though without completely reaching its final equilibrium position within the time scale investigated here. In the very first time of the ionization step, k_{-2}[AcO^-] could be neglected in front of k_2 because of the low AcO^- concentration (≪1 mM). The value of k_2 was then calculated from the initial slope of the curve in Figure 2b (Table 2, entry 2) taking into account the value of the theoretical final conductivity κ_{lim} determined above (Figure 2b).[8a] The initial slope did not depend on the concentration of **1** within the investigated concentration range, confirming a zero-order reaction in **1** for the ionization step. The value of k_{-2} could not be determined because of a too fast reaction between **5a**$^+BF_4^-$ and AcO^- even at low acetate concentrations (1 mM each).

Therefore, in DMF, the reaction of **1** with the Pd^0 complex generated from $Pd^0(dba)_2$ and 2PPh_3 is reversible and proceeds in two successive equilibria (Scheme 3) after the initial formation of *S*$Pd^0(PPh_3)_2$. A fast overall complexation step is followed by a slower ionization step: k_1^{app}[**1**] > k_2 as soon as [**1**] > 0.2 mM.

In contrast to what was observed in DMF, the ionization went to completion in acetonitrile, since the final value of the conductivity κ_{lim} was equal to the expected one, as determined independently.[8b] The rate constant k_2 of the ionization step was then determined (Table 2, entry 3, Figure S2 in Supporting Information). The ionization was faster in acetonitrile than in DMF.

Reaction of (*E*)-1,3-Diphenyl-3-acetoxyprop-1-ene (1) with $Pd^0(PPh_3)_4$. Further Evidence of the Formation of the Neutral Intermediate Complex (η^2-PhCH=CH-CH(Ph)-OAc)$Pd^0(PPh_3)_2$, 6a. It is known that $Pd^0(PPh_3)_4$ dissociates in DMF to give $Pd^0(PPh_3)_3$ as the major complex, whereas the minor complex *S*$Pd^0(PPh_3)_2$ is the active species in oxidative additions.[9] The reaction of $Pd^0(PPh_3)_4$ (20 mM) with (*E*)-1,3-diphenyl-3-acetoxyprop-1-ene (**1**) (22 equiv) was

Scheme 6

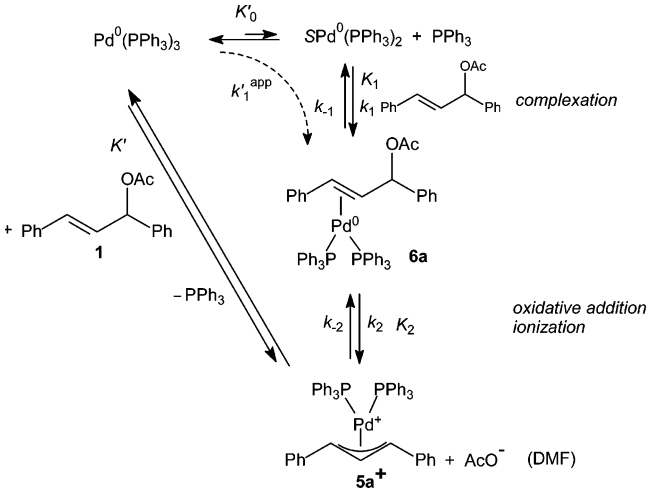

monitored by ^{31}P NMR spectroscopy in DMF containing 10% acetone-d_6. The broad signal characteristic of the fast equilibrium involving $Pd^0(PPh_3)_3$, *S*$Pd^0(PPh_3)_2$, and PPh_3 at 10.6 ppm[6a] was not detected, but the two doublets of the intermediate Pd^0 complex **6a** were observed at 24.97 and 24.61 ppm, as when the reaction was performed from $Pd^0(dba)(PPh_3)_2$ (vide supra). The singlet of the cationic complex **5a**$^+$ appeared after 1 day. This experiment shows that the ionization step was much slower than the complexation step. The intermediate complex (η^2-PhCH=CH−CH(Ph)-OAc)$Pd^0(PPh_3)_2$, **6a**, accumulated and could then be characterized by ^{31}P NMR spectroscopy. The mechanism of the reaction may then be described as in Scheme 6 since the reversibility of the ionization and complexation steps has already been established in the reaction of **1** with $Pd^0(dba)(PPh_3)_2$ (Scheme 3).

The reaction of **1** with $Pd^0(PPh_3)_4$ (1 mM) was monitored by UV spectroscopy in DMF. The absorbance of $Pd^0(PPh_3)_3$ at λ_{max} = 320 nm[6b] decreased and stabilized upon successive addition of **1** up to 16 equiv (Figure 4a), attesting that $Pd^0(PPh_3)_3$ and **1** were involved in an equilibrium.

However, the absorbance of $Pd^0(PPh_3)_3$ at 320 nm never reached a residual value as observed for $Pd^0(dba)(PPh_3)_2$ (vide supra, Figure 2a) because a new band developed at ca. 340 nm (Figure 4a).[10] This band was assigned to the intermediate Pd^0 complex **6a** which accumulated, due to its very slow ionization to the cationic complex **5a**$^+$. This was further confirmed by the following experiment. The cationic complex **5a**$^+BF_4^-$ (1

(9) Fauvarque, J. F.; Pflüger, F.; Troupel, M. *J. Organomet. Chem.* **1981**, *208*, 419.

(10) It is only when PhI was added that all the $Pd^0(PPh_3)_3$ disappeared (Figure 4a) due to a faster reaction of PhI with the Pd^0 involved in the equilibrium with **1**.

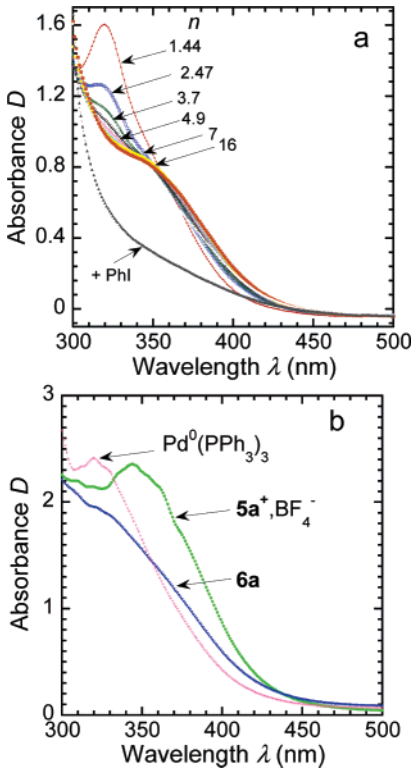

Figure 4. UV spectroscopy performed in DMF in a 1 mm length cell at 25 °C. (a) $Pd^0(PPh_3)_4$ (1 mM) after successive additions of PhCH=CH-CH(Ph)-OAc (as indicated by the arrows, n is the total number of equivalents added). PhI (50 equiv) was added at the end of the reaction as indicated by the arrow to observe the total disappearance of the initial $Pd^0(PPh_3)_4$ complex. (b) [(η^3-PhCH-CH-CHPh)Pd-$(PPh_3)_2$]$^+BF_4^-$ (**5a**$^+BF_4^-$) (1 mM); [(η^2-PhCH=CH-CH(Ph)-OAc)$Pd^0(PPh_3)_2$, **6a**, generated by addition of nBu$_4$NOAc (1 mM) to **5a**$^+BF_4^-$. $Pd^0(PPh_3)_3$ generated after addition of PPh_3 (2 mM) to the previous solution.

mM) in DMF exhibited an absorption band at λ_{max} = 350 nm (Figure 4b). After addition of 1 equiv of nBu$_4$-NOAc, the absorption band of **5a**$^+BF_4^-$ immediately disappeared and a new band appeared at λ_{max} = 330 nm (Figure 4b). After further addition of PPh_3, the absorption band at λ_{max} = 320 nm characteristic of Pd^0-$(PPh_3)_3$ was restored (Figure 4b). This shows that the reaction of AcO^- with the cationic complex **5a**$^+$ resulted in the fast formation of the intermediate Pd^0 complex **6a** absorbing at λ_{max} = 330 nm, whose allylic acetate ligand **1** was then displaced by further addition of excess PPh_3. The intermediate Pd^0 complex **6a** could not be detected by UV spectroscopy starting from $Pd^0(dba)$-$(PPh_3)_2$ due to overlapping with the absorbance of dba (Figure 2a). When starting from $Pd^0(PPh_3)_4$, the intermediate complex (η^2-PhCH=CH-CH(Ph)-OAc)$Pd^0(PPh_3)_2$, **6a**, could then be characterized by UV spectroscopy in addition to ^{31}P NMR.

Complexation Step: Kinetic and Thermodynamic Data. Since the ionization step is much slower than the complexation step within the concentration range of **1** investigated here, it can be neglected and the equilibrium constant K'_0K_1 = [**6a**][PPh_3]/[**1**][Pd^0-$(PPh_3)_3$] of the overall complexation step (Scheme 7) was determined using the UV data presented in Figure 4a (Table 2, entry 1, see Figure S3a in the Supporting Information).

Scheme 7. Overall Complexation Step

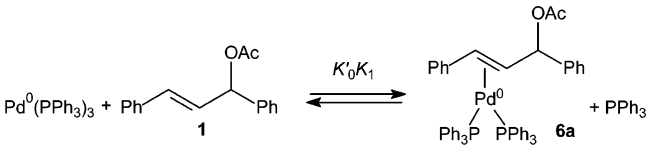

Comparison to the value of K_0K_1 determined for Pd^0-$(dba)(PPh_3)_2$ (Table 2, entry 2) allows the determination of the ratio K'_0/K_0 = 9.6 (DMF, 25° C). This shows that the $SPd^0(PPh_3)_2$ concentration in the equilibrium with $Pd^0(PPh_3)_3$ is ca. 10 times higher than that formed in the equilibrium with $Pd^0(dba)(PPh_3)_2$ at identical initial Pd^0 concentrations. This result is fully coherent with that already established during our previous investigation of the kinetics of the oxidative addition with PhI for which K'_0/K_0 = 8.6 (DMF, 20 °C) was found.[6a] This confirms that dba is a much better ligand for the moiety $Pd^0(PPh_3)_2$ than PPh_3.

The kinetics of the overall complexation step (see $k'_1{}^{app}$ in Scheme 6) was monitored by UV spectroscopy by recording the decrease of the absorbance of Pd^0-$(PPh_3)_3$ (C_0 = 1 mM) at 320 nm *versus time* in the presence of large amounts of **1** (nC_0 > 0.015 M), i.e., upon conditions of an overall irreversible step. The kinetic law is given in eq 6 similar to eq 5.

$$2\ln x - x + 1 = -K'_0k_1[\mathbf{1}]t/C_0 = -k_{exp}t = k'_1{}^{app}[\mathbf{1}]t \quad (6)$$

The values of $k'_1{}^{app}$ and K'_0k_1 were determined (Table 2, entry 1) using the same procedure as above for Pd-$(dba)_2$ associated to $2PPh_3$ (Figure S3b in the Supporting Information).

Ionization Step. This step (Scheme 5) is common to both systems whatever the Pd^0 precursor, $Pd^0(PPh_3)_4$ or $Pd^0(dba)_2$, and $2PPh_3$ with k_2 already determined above (Table 2, entry 2). It was found to be slower than the overall complexation step: $k'_1{}^{app}$[**1**] > k_2 as soon as [**1**] > 4 μM.

Reaction of (*E*)-1,3-Diphenyl-3-acetoxyprop-1-ene (1) with the Pd^0 Complex Generated from $Pd^0(dba)_2$ and dppb. As previously reported, the complex $Pd^0(dba)$(dppb) is generated quantitatively in DMF from $Pd^0(dba)_2$ (1 mM) and 1 equiv of dppb after a slow reaction (45 min) because of the formation of the intermediate complex $Pd^0(dppb)_2$ (Scheme 8).[11]

Scheme 8. Mechanism of the Formation of $Pd^0(dba)(dppb)$

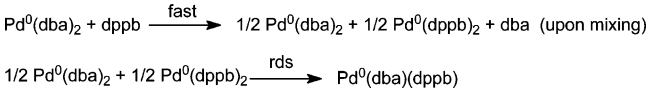

This reaction was investigated by ^{31}P NMR spectroscopy performed in DMF containing acetone-d_6. The singlet of $Pd(dppb)_2$ at 28.91 ppm progressively disappeared to give two broad singlets at 20.6 and 17.7 ppm characteristic of $Pd^0(dba)(dppb)$.[11] When 69 equiv of (*E*)-1,3-diphenyl-3-acetoxypropene, **1**, was added, two close singlets appeared at 20.66 and 20.44 ppm as well as one singlet at 23.14 ppm. The latter characterizes the cationic complex **5b**$^+$(η^3-PhCH-CH-CHPh)Pd(dppb)$^+$,

(11) Amatore, C.; Broeker, G.; Jutand, A.; Khalil, F. *J. Am. Chem. Soc.* **1997**, *119*, 5176.

Scheme 9

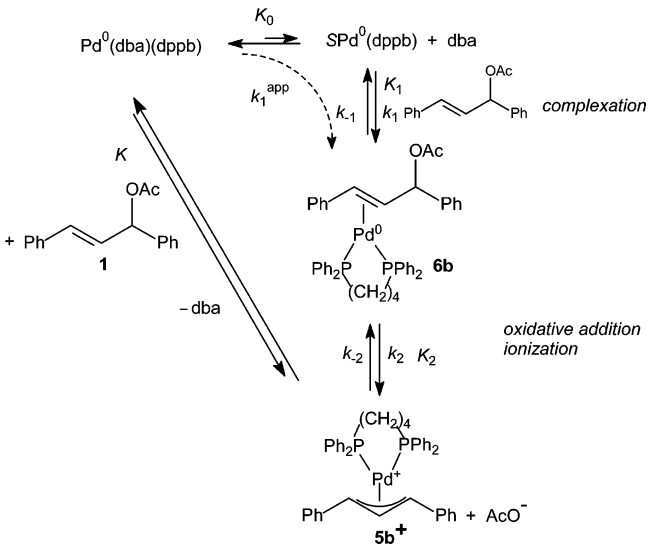

which was independently synthesized by reacting dppb with $[(\eta^3\text{-PhCH-CH-CHPh})Pd(\mu\text{-Cl})]_2$ (dppb/Pd = 1) in the presence of $NaBF_4$, in a reaction similar to that described in eq 3. The two close singlets generated in the very first step of the reaction were assigned to the intermediate Pd^0 complex: (η^2-PhCH=CH-CH(Ph)-OAc)-Pd^0(dppb), **6b** (Scheme 9). Complex **6b** should be characterized by two doublets, but since they were very close, only two close singlets were then observed.

Evidence of the Reversibility of the Oxidative Addition. The formation of the cationic complex **5b**$^+$ was monitored by conductivity measurements in DMF after addition of n = 32.1 equiv of **1** to Pd^0(dba)(dppb) (C_0 =1 mM), quantitatively generated from $Pd^0(dba)_2$ (1 mM) and dppb (1 mM). The conductivity increased with time (Figure 5, 3000 < t < 20 000 s) to reach a limiting value that was close to that expected for **5b**$^+$AcO$^-$ (1 mM) (κ_{lim} = 65 μS cm^{-1}, vide infra). What was observed in Figure 5 is then the nearly irreversible formation of the cationic complex **5b**$^+$ from complex **6b**. In another experiment involving n = 24 equiv of **1**, it was observed that the conductivity was not modified by the successive addition of **1** (10.4 equiv and then 6.4 equiv) in the course of the reaction. Consequently, the kinetics of formation of **5b**$^+$AcO$^-$ did not depend on the concentration of **1** (zero-order reaction), which means that whatever the concentration of **1** investigated here (>24 mM), the ionization step was always slower than the overall complexation step and was closely kinetically irreversible.

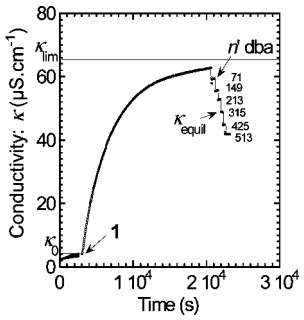

Figure 5. Conductivity measurements in DMF versus time of $[(\eta^3\text{-PhCH-CH-CHPh})Pd(dppb)]^+AcO^-$ (**5b**$^+$AcO$^-$) generated in the reaction of PhCH=CH-CH(Ph)-OAc (32.1 mM) with Pd^0(dba)(dppb) (1 mM) formed in situ by reacting $Pd^0(dba)_2$ (1 mM) and dppb (1 mM) at 30 °C. Once the reaction was almost over (t = 20 000 s), dba was successively added (n' is the total number of equivalents of added dba). κ_{lim} is the conductivity of **5b**$^+$AcO$^-$ (1 mM) in DMF at 25 °C, as determined from the kinetics of the ionization step.[13]

Scheme 10

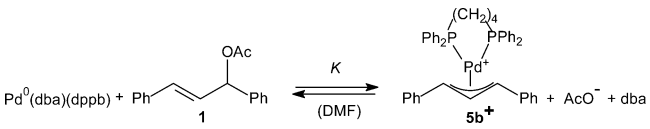

Ionization Step: Kinetic Data. As explained above, the increase of the conductivity with time (3000 < t < 20 000 s in Figure 5) gives the kinetics of the ionization of the intermediate complex **6b** to the cationic complex **5b**$^+$AcO$^-$ in DMF. Since the experiment was stopped slightly before the ionization was over, the kinetics was treated using the Guggenheim method (Figure S4b in the Supporting Information), which allowed the determination of k_2 (Table 2, entry 4).[12,13] As expected, k_2 does not depend on the concentration of **1**, which confirms the mechanism of Scheme 9 with an overall complexation step faster than the ionization step, which is the rate-determining step of the overall process: k_1^{app}[**1**] > k_2 as soon as [**1**] > 1 mM.

The values of all the equilibrium and rate constants determined in this work are gathered in Table 2 (entries 1−4) for the different precursors of Pd^0 complexes investigated here. Once more, we observe that not only the *ligand* of the Pd^0 complex but also the *precursor* of the Pd^0 complex affect the overall thermodynamics and kinetics of the reactions.

As far as the *complexation* step is concerned, the reactivity order is the following:

Reversibility of the Ionization Step: Kinetic Data. The reversibility of the ionization step could nevertheless be established upon addition of successive aliquots of dba (n' equiv) after the almost quantitative formation of **5b**$^+$ (Figure 5, t > 20 000 s). This resulted in successive decreases of the conductivity, reflecting the corresponding decrease of the concentration of the ionic species. Since the reversibility was induced by addition of dba, the overall equilibrium constant $K = K_0K_1K_2 = [\mathbf{5b}^+][AcO^-][dba]/[Pd^0(dba)(dppb)][\mathbf{1}]$ (Scheme 10) could be determined (Table 2, entry 4, Figure S4a in the Supporting Information) using the conductivity data shown at t > 20 000 s in Figure 5.

Complexation Step: Kinetic Data. The kinetics of the reaction of Pd^0(dba)(dppb) (C_0 = 1 mM) with **1** (n equiv) was monitored by UV spectroscopy in DMF by recording the decrease of its absorbance at λ_{max} = 385 nm under conditions where the overall complexation step was irreversible (n > 10), as performed above for $Pd^0(dba)(PPh_3)_2$ (vide supra). The values of K_0k_1 and k_1^{app} (Scheme 9) were determined (Table 2, entry 4, Figure S5 in the Supporting Information).

---

(12) Guggenheim, E. A. *Philos. Mag.* **1936**, *22*, 322

(13) Using this value of k_2, one can evaluate that $t_{1/2}$ = 2340 s with $\kappa_{1/2}$ = 30.7 μS cm^{-1}. The theoretical conductivity of **5b**$^+$AcO$^-$ (1 mM in DMF at 30 °C) is then 61.4 μS cm^{-1}. Taking into account the residual conductivity κ_0 = 4 μS cm^{-1}, one predicts a final experimental conductivity of 65.4 μS cm^{-1} (κ_{lim} in Figure 5), for a total displacement of the equilibrium. This shows a posteriori that the ionization reaction (Figure 5) was indeed almost complete at t = 20 000 s, before the addition of dba.

For k_1^{app}: $Pd^0(PPh_3)_4 > Pd^0(dba)_2 + 2\ PPh_3 > Pd^0(dba)_2 + 1\ dppb$

This reactivity order is very reminiscent of that observed for the oxidative addition of PhI.[6a,c,11] Even if a complexation of a C=C bond strongly differs from an oxidative addition, similar arguments may explain the difference of reactivity. That is to say (i) the higher $Pd^0(PPh_3)_2$ concentration in its equilibrium with $Pd^0(PPh_3)_3$ than in its equilibrium with $Pd^0(dba)(PPh_3)_2$[6a] and (ii) the higher $Pd^0(PPh_3)_2$ concentration in its equilibrium with $Pd^0(dba)(PPh_3)_2$ than the $Pd^0(dppb)$ concentration in its equilibrium with $Pd^0(dba)(dppb)$.[11] Moreover, dppb is more electron rich than PPh_3. This disfavors the complexation of the C=C bond of **1** to the Pd^0 moiety.

As far as the *ionization* step from the neutral complexes **6a** or **6b** is concerned, only the effect of the ligand has to be taken into consideration with the following reactivity order (Table 2):

For k_2: dppb > PPh_3

In all cases investigated here, the ionization was found to be slower than the complexation step, and a complete ionization reaction was observed only for the dppb ligand under comparable experimental conditions in DMF, which suggests that the reverse reaction, i.e., the attack of the acetate ion on the cationic complex, follows the reverse reactivity order (Table 2):

For k_{-2}: PPh_3 > dppb

The ionization step may be considered as an oxidative addition, which should be favored by the more electron-rich dppb ligand, whereas the reverse reaction, nucleophilic attack of the acetate ion onto the cationic complex, will be favored for the more electron-poor PPh_3.

The values of the equilibrium and rate constants of the reaction of PhCH=CH-CH(Ph)-OAc with $Pd^0(dba)(dppp)$ generated from $Pd(dba)_2$ and 1 dppp (Table 2, entry 4) in DMF can be compared to those obtained for CH_2=CH-CH_2-OAc reported in a previous work[2b] (Table 2, entry 5). The overall equilibrium constants K are very similar. However, for similar concentrations of the reagents, the overall complexation is slower for PhCH=CH-CH(Ph)-OAc than for CH_2=CH-CH_2-OAc (compare K_0k_1 in entries 4 and 5). The ionization step is also slower (compare k_2 in entries 4 and 5). This is due to steric hindrance induced by the two phenyl groups, which disfavors both the complexation of the C=C bond and the release of the acetate ion as in an S_N2 substitution. Since the overall equilibrium constant K is similar for both allylic acetates, this means that the overall backward reaction is also slower for PhCH=CH-CH(Ph)-OAc than for CH_2=CH-CH_2-OAc. The value of $k_{-1}k_{-2}$ can be calculated from the known values of K and $K_0k_1k_2$ since $K = K_0k_1k_2/k_{-1}k_{-2}$. One obtains $k_{-1}k_{-2} = 7.5 \times 10^{-6}\ M^{-1}\ s^{-2}$ for PhCH=CH-CH(Ph)-OAc and $k_{-1}k_{-2} = 8 \times 10^{-2}\ M^{-1}\ s^{-2}$ for CH_2=CH-CH_2-OAc. One would expect a faster decomplexation step from (η^2-PhCH=CH-CH(Ph)-OAc)Pd^0(dppb) than from (η^2-CH_2=CH-CH_2-OAc)Pd^0(dppb) due to steric decompression; that is, one expects k_{-1} to be higher for PhCH=CH-CH(Ph)-OAc than for CH_2=CH-CH_2-OAc. This suggests that the value of k_{-2}, i.e., the rate constant of the attack of the acetate ion on [(η^3-PhCH-CH-CHPh)Pd(dppb)]$^+$, must be considerably lower than that on [(η^3-CH_2-CH-CH_2)-Pd(dppb)]$^+$, due also to steric hindrance.

Conclusion

In DMF, the reaction of (*E*)-PhCH=CH-CH(Ph)-OAc with Pd^0L_2 complexes (L = PPh_3 or L_2 = dppb) is reversible and proceeds in two steps: complexation followed by ionization leading to cationic complexes [(η^3-PhCH-CH-CHPh)PdL_2]$^+AcO^-$. The intermediate Pd^0 complexes, (η^2-PhCH=CH-CH(Ph)-OAc)Pd^0L_2, have been characterized for the first time in DMF. The overall complexation step starting from $Pd^0(PPh_3)_3$, $Pd^0(dba)(PPh_3)_2$, or $Pd^0(dba)$(dppb) is faster than the ionization step, which is rate-determining. The rate of the complexation step depends both on the ligand and on the Pd^0 precursor. In DMF, for the precursor $Pd(dba)_2$, the ionization step is faster considering dppb compared to PPh_3. Considering the same dppb ligand and the same precursor $Pd(dba)_2$, with identical concentrations of the reagents, the formation of the cationic complex from PhCH=CH-CH(Ph)-OAc is considerably slower than with the simple allyl acetate CH_2=CH-CH_2-OAc.

Work is in progress to compare the rate of formation of the cationic complexes with the rate of the nucleophilic attack. Some preliminary results on the kinetics of the nucleophilic attack[14] of morpholine on the cationic complex **5a**$^+$ indicate that for identical concentrations of **1** and morpholine the nucleophilic attack is considerably faster than the overall formation of the cationic complex **5a**$^+$, which is then turnover limiting.

Experimental Section

General Procedures. ^{31}P NMR spectra were recorded in acetone-d_6 or in DMF containing 10% acetone-d_6 on a Bruker spectrometer (101 MHz) with H_3PO_4 as an external reference. UV spectra were recorded on a mc^2 Safas Monaco spectrometer. Conductivity measurements were performed on a Tacussel CDM210 conductivity meter (cell constant = 1 cm^{-1}). All experiments were performed under argon atmosphere.

Chemicals. DMF was distilled from calcium hydride under vacuum and kept under argon. dba, PPh_3, and dppb were commercial. $Pd^0(dba)_2$,[15] (*E*)-1,3-diphenyl-3-acetoxyprop-1-ene (**1**),[16] and [Pd(η^3-Ph-CH-CH−CH-Ph)(μ-Cl)]$_2$[7b] were prepared according to described procedures.

Typical Procedure for UV Experiments. From a mother solution of 10 mL of DMF containing 8.6 mg (30 μmol) of $Pd^0(dba)_2$ and 15.7 mg (60 μmol) of PPh_3, a 300 μL aliquot was transferred under argon to the thermostated UV cell (1 mm length) and UV was performed. It was followed by the addition of known amounts of (*E*)-1,3-diphenyl-3-acetoxyprop-1-ene from a mother solution (see Figure 3a). The UV was performed immediately after hand-shaking the cell. When necessary, the dilution was taken into account.

(14) (a) Amatore, C.; Jutand, A.; Mensah, L. **2004**, unpublished results. For the investigation of the kinetics of the nucleophilic attack on cationic (η^3-allyl)palladium complexes see also: (b) Antonaroli, S.; Crociani, B. *J. Organomet. Chem.* **1998**, *560*, 137. (c) Kuhn, O.; Mayr, H. *Angew. Chem., Int. Ed.* **1999**, *38*, 343. (d) Canovese, L.; Visentin, F.; Chessa, G.; Niero, G.; Uguagliati, P. *Inorg. Chim. Acta* **1999**, *293*, 44. (e) Crociani, B.; Antonaroli, S.; Canovese, L.; Visentin, F.; Uguagliati, P. *Inorg. Chim. Acta* **2001**, *315*, 172. (f) Cantat, T.; Génin, E.; Giroud, C.; Meyer, G.; Jutand, A. *J. Organomet. Chem.* **2003**, *687*, 365.

(15) Takahashi, Y.; Ito, Ts.; Ishii, Y. *J. Chem. Soc., Chem. Commun.* **1970**, 1065.

(16) Leung, W.; Cosway, S.; Jones, R. H. V.; McCann, H.; Wills, M. *J. Chem. Soc., Perkins Trans. 1* **2001**, 2288.

In another experiment (see Figure 2a), from a mother solution of 2 mL of DMF containing 2.8 mg (2 μmol, 1 mM) of **5a**$^+BF_4^-$, a 300 μL aliquot was transferred under argon to the thermostated UV cell (1 mm length) and UV was performed. It was followed by the addition of 10 equiv of nBu$_4$NOAc (20 μL from a mother solution containing 105.5 mg of nBu$_4$NOAc in 2 mL of DMF). UV was performed. Two equivalents of dba (10 μL from a mother solution containing 32.8 mg of dba in 2 mL of DMF) was then added and UV was performed.

Typical Procedure for Conductivity Measurements. In a thermostated cell containing a solution of 17.2 mg (30 μmol) of Pd^0(dba)$_2$ and 15.7 mg (60 μmol) of PPh_3 in 10 mL of DMF was added known amounts of (*E*)-1,3-diphenyl-3-acetoxyprop-1-ene. The conductivity was recorded with time using a computerized homemade program.[4]

Synthesis of [(η^3-Ph-CH-CH-CH-Ph)Pd(PPh_3)$_2$]$^+BF_4^-$.[7c] A solution of 763 mg (2.91 mmol) of PPh_3 in 10 mL of acetone was added to a solution of 384 mg (0.728 mmol) of [Pd[(η^3-Ph-CH-CH-CH-Ph)(μ-Cl)]$_2$ in 13 mL of acetone, followed by a solution of 799 mg (7.3 mmol) of $NaBF_4$ in 13 mL of water. A yellow precipitate appeared. After filtration, the solid was washed with water and diethyl ether and dried under vacuum. [(η^3-Ph-CH-CH-CH-Ph)Pd(PPh_3)$_2$]$^+BF_4^-$ (798 mg, 60%) was collected. The product was crystallized from dichloromethane and pentane as a cosolvent. Monocrystals were formed (see Figure 1 for the X-ray structure). ^{1}H NMR (250 MHz, $CDCl_3$, TMS): δ 5.72 (ddd, J_{HH} = 11 Hz, J_{PH} = 6 Hz, J_{PH} = 6 Hz, 2H, CH_{anti}), 6.35 (t, J_{HH} = 14 Hz, 1H, central H), 6.78 (m, 10H, Ph), 7.05 (m, 18H, Ph of PPh_3), 7.2 (m, 12H, Ph of PPh_3). ^{31}P NMR (101 MHz, DMF + acetone-d_6 10%): δ 28.2 (s); (101 MHz, $CDCl_3$); δ 23.36 (s). FAB-MS (MB 001): m/z = 823 [M]$^+$, 630 [M − (Ph-CH-CH-CH-Ph)], 561 [M − PPh_3].

Synthesis of [(η^3-Ph-CH-CH-CH-Ph)Pd(dppb)]$^+$BF4$^-$. The procedure was the same as that used above for PPh_3. [(η^3-Ph-CH-CH-CH-Ph)Pd(dppb)]$^+BF_4^-$ (260 mg, 90%) was collected. ^{1}H NMR (250 MHz, $CDCl_3$, TMS): δ 1.60−12.1 (m, 4H, CH_2-CH_2 of dppb), 2.45 (dm, J_{PH} = 6.7 Hz, 4H, CH_2-P), 5.35 (ddd, 2H, J_{HH} = 12 Hz, J_{PH} = 6 Hz, J_{PH} = 6 Hz, H_{anti}), 6.33 (t, 1H, J_{HH} = 12 Hz, central H), 6.75−6.9 (m, 6H, Ph), 6.9−7.1 (m, 4H, Ph), 7.2−7.5 (m, 20 H, Ph of PPh_3). ^{31}P NMR NMR (101 MHz, DMF + acetone-d_6 10%): δ 23.16 (s); (101 MHz, $CDCl_3$) δ 21.35 (s). FAB-MS (MB 001): m/z = 725 [M]$^+$, 532 [M − (Ph-CH-CH-CH-Ph)].

Acknowledgment. This work has been supported in part by the Centre National de la Recherche Scientifique (UMR CNRS-ENS-UPMC 8640) and the Ministère de la Recherche (Ecole Normale Supérieure). We thank Johnson Matthey for a generous loan of sodium tetrachloropalladate.

Supporting Information Available: Graphs for the determination of equilibrium constants, rate constants, and X-ray data. This material is available free of charge via the Internet at http://pubs.acs.org.

OM049420D